[7] M. Ono, J. Matsubara, K. Honda, T. Sakuma, T. Hashiguchi, H. Nose et al. Prolyl 4-hydroxylation of alpha-fibrinogen: a novel protein modification revealed by plasma proteomics, J Biol Chem 284 (2009), 29041-29049.
[8] A. Negishi, M. Ono, Y. Handa, H. Kato, K. Yamashita, K. Honda et al. Large-scale quantitative clinical proteomics by label-free liquid chromatography and mass spectrometry, Cancer Sci 100 (2009), 514-519.
[9] J. Matsubara, M. Ono, A. Negishi, H. Ueno, T. Okusaka, J. Furuse et al. Identification of a predictive biomarker for hematologic toxicities of gemcitabine, J Clin Oncol 27 (2009), 2261-2268.
[10] A. Yokomizo, K. Yamamoto, K. Furuno, M. Shiota, K. Tatsugemi, K. Kuroiwa et al. Histopathologic subtype-specific genomic profiles of renal cell carcinomas identified by high-resolution whole-genome single nucleotide polymorphism array analysis, Oncol Lett 1 (2010), 1073-1078.
[11] TNM Classification of Malignant Tumours. John Wiley and Sons Ltd 2009.
[12] M. Shitashige, R. Satow, K. Honda, M. Ono, S. Hirohashi, T. Yamada. Regulation of Wnt signaling by the nuclear pore complex, Gastroenterology 134 (2008), 1961-1971, 1971 e1961-1964.
[13] J.D. Storey, R. Tibshirani. Statistical significance for genome-wide studies, Proc Natl Acad Sci USA 100 (2003), 9440-9445.
[14] S.M. Albelda. Role of integrins and other cell adhesion molecules in tumor progression and metastasis, Lab Invest 68 (1993), 4-17.
[15] R.O. Hynes, K.M. Yamada. Fibronectins: multifunctional modular glycoproteins, J Cell Biol 95 (1982), 369-377.
[16] R. Pankov, K.M. Yamada. Fibronectin at a glance, J Cell Sci 115 (2002), 3861-3863.
[17] H. Ro. Fibronectins. Berlin, Heidelberg, New York: Springer.
[18] W. Brenner, S. Gross, F. Steinbach, S. Horn, R. Hohenfellner, J.W. Thuroff. Differential inhibition of renal cancer cell invasion mediated by fibronectin, collagen IV and laminin, Cancer Lett 155 (2000), 199-205.
[19] J. Lohi, T. Tani, I. Leivo, A. Linnala, L. Kangas, R.E. Burgeson et al. Expression of laminin in renal-cell carcinomas, renal-cell carcinoma cell lines and xenografts in nude mice, Int J Cancer 68 (1996), 364-371.
[20] J. Murata, I. Saiki, J. Yoneda, I. Azuma. Differences in chemotaxis to fibronectin in weakly and highly metastatic tumor cells, Jpn J Cancer Res 83 (1992), 1327-1333.
[21] A. Hegele, A. Heidenreich, J. Kropf, R. von Knobloch, Z. Varga, R. Hofmann et al. Plasma levels of cellular fibronectin in patients with localized and metastatic renal cell carcinoma, Tumour Biol 25 (2004), 111-116.
[22] S. Waalkes, F. Atschekzei, M.W. Kramer, J. Hennenlotter, G. Vetter, J.U. Becker et al. Fibronectin 1 mRNA expression correlates with advanced disease in renal cancer, BMC Cancer 10 (2010), 503.

Supplemental material

MS/MS Fragmentation of **RPGGEPSPEGTTGQSYNQYSQR**
Found in **FINC_HUMAN**, Fibronectin OS=Homo sapiens GN=FN1 PE=1 SV=3
Match to Query 1: 2395.118583 from(799.380137,3+)

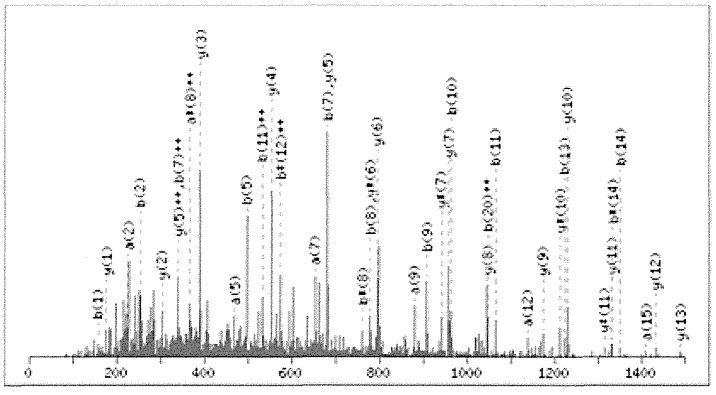

Monoisotopic mass of neutral peptide Mr(calc): 2395.0789
Ions Score: 84 **Expect:** 6.3e-008
Matches (Bold Red): 41/252 fragment ions using 78 most intense peaks

#	a	a++	a*	a*++	b	b++	b*	b*++	Seq.	y	y++	y*	y*++	#
1	129.1135	65.0604	112.0869	56.5471	157.1084	79.0578	140.0818	70.5446	R					22
2	226.1662	113.5868	209.1397	105.0735	254.1612	127.5842	237.1346	119.0709	P	2239.985	1120.4962	2222.9585	1111.9829	21
3	283.1877	142.0975	266.1612	133.5842	311.1826	156.0949	294.1561	147.5817	G	2142.9323	1071.9698	2125.9057	1063.4565	20
4	340.2092	170.6082	323.1826	162.0949	368.2041	184.6057	351.1775	176.0924	G	2085.9108	1043.459	2068.8843	1034.9458	19
5	469.2518	235.1295	452.2252	226.6162	497.2467	249.127	480.2201	240.6137	E	2028.8894	1014.9483	2011.8628	1006.435	18
6	566.3045	283.6559	549.278	275.1426	594.2994	297.6534	577.2729	289.1401	P	1899.8468	950.427	1882.8202	941.9137	17
7	653.3365	327.1719	636.31	318.6586	681.3315	341.1694	664.3049	332.6561	S	1802.794	901.9006	1785.7674	893.3874	16
8	750.3893	375.6983	733.3628	367.185	778.3842	389.6958	761.3577	381.1825	P	1715.762	858.3846	1698.7354	849.8713	15
9	879.4319	440.2196	862.4054	431.7063	907.4268	454.217	890.4003	445.7038	E	1618.7092	809.8582	1601.6827	801.345	14
10	936.4534	468.7303	919.4268	460.217	964.4483	482.7278	947.4217	474.2145	G	1489.6666	745.3369	1472.6401	736.8237	13
11	1037.501	519.2542	1020.4745	510.7409	1065.496	533.2516	1048.4694	524.7383	T	1432.6451	716.8262	1415.6186	708.3129	12
12	1138.5487	569.778	1121.5222	561.2647	1166.5436	583.7755	1149.5171	575.2622	T	1331.5975	666.3024	1314.5709	657.7891	11
13	1195.5702	598.2887	1178.5436	589.7755	1223.5651	612.2862	1206.5386	603.7729	G	1230.5498	615.7785	1213.5232	607.2653	10
14	1323.6288	662.318	1306.6022	653.8047	1351.6237	676.3155	1334.5971	667.8022	Q	1173.5283	587.2678	1156.5018	578.7545	9
15	1410.6608	705.834	1393.6342	697.3208	1438.6557	719.8315	1421.6292	711.3182	S	1045.4697	523.2385	1028.4432	514.7252	8
16	1573.7241	787.3657	1556.6976	778.8524	1601.719	801.3632	1584.6925	792.8499	Y	958.4377	479.7225	941.4112	471.2092	7
17	1687.7671	844.3872	1670.7405	835.8739	1715.762	858.3846	1698.7354	849.8713	N	795.3744	398.1908	778.3478	389.6776	6
18	1815.8256	908.4165	1798.7991	899.9032	1843.8205	922.4139	1826.794	913.9006	Q	681.3315	341.1694	664.3049	332.6561	5

Fig. S1. Mascot report of one representative fragment of FN1.

```
1       MLRGPGPGLL LLAVQCLGTA VPSTGASKSK RQAQQMVQPQ SPVAVSQSKP
51      GCYDNGKHYQ INQQWERTYL GNALVCTCYG GSRGFNCESK PEAEETCFDK
101     YTGNTYRVGD TYERPKDSMI WDCTCIGAGR GRISCTIANR CHEGGQSYKI
151     GDTWRRPHET GGYMLECVCL GNGKGEWTCK PIAEKCFDHA AGTSYVVGET
201     WEKPYQGWMM VDCTCLGEGS GRITCTSRNR CNDQDTRTSY RIGDTWSKKD
251     NRGNLLQCIC TGNGRGEWKC ERHTSVQTTS SGSGPFTDVR AAVYQPQPHP
301     QPPPYGHCVT DSGVVYSVGM QWLKTQGNKQ MLCTCLGNGV SCQETAVTQT
351     YGGNSNGEPC VLPFTYNGRT FYSCTTEGRQ DGHLWCSTTS NYEQDQKYSF
401     CTDHTVLVQT QGGNSNGALC HFPFLYNNHN YTDCTSEGRR DNMKWCGTTQ
451     NYDADQKFGF CPMAAHEEIC TTNEGVMYRI GDQWDKQHDM GHMMRCTCVG
501     NGRGEWTCIA YSQLRDQCIV DDITYNVNDT FHKRHEEGHM LNCTCFGQGR
551     GRWKCDPVDQ CQDSETGTFY QIGDSWEKYV HGVRYQCYCY GRGIGEWHCQ
601     PLQTYPSSSG PVEVFITETP SQPNSHPIQW NAPQPSHISK YILRWRPKNS
651     VGRWKEATIP GHLNSYTIKG LKPGVVYEGQ LISIQQYGHQ EVTRFDFTTT
701     STSTPVTSNT VTGETTPFSP LVATSESVTE ITASSFVVSW VSASDTVSGF
751     RVEYELSEEG DEPQYLDLPS TATSVNIPDL LPGRKYIVNV YQISEDGEQS
801     LILSTSQTTA PDAPPDPTVD QVDDTSIVVR WSRPQAPITG YRIVYSPSVE
851     GSSTELNLPE TANSVTLSDL QPGVQYNITI YAVEENQEST PVVIQQETTG
901     TPRSDTVPSP RDLQFVEVTD VKVTIMWTPP ESAVTGYRVD VIPVNLPGEH
951     GQRLPISRNT FAEVTGLSPG VTYYFKVFAV SHGRESKPLT AQQTTKLDAP
1001    TNLQFVNETD STVLVRWTPP RAQITGYRLT VGLTRRGQPR QYNVGPSVSK
1051    YPLRNLQPAS EYTVSLVAIK GNQESPKATG VFTTLQPGSS IPPYNTEVTE
1101    TTIVITWTPA PRIGFKLGVR PSQGGEAPRE VTSDSGSIVV SGLTPGVEYV
1151    YTIQVLRDGQ ERDAPIVNKV VTPLSPPTNL HLEANPDTGV LTVSWERSTT
1201    PDITGYRITT TPTNGQQGNS LEEVVHADQS SCTFDNLSPG LEYNVSVYTV
1251    KDDKESVPIS DTIIPAVPPP TDLRFTNIGP DTMRVTWAPP PSIDLTNFLV
1301    RYSPVKNEED VAELSISPSD NAVVLTNLLP GTEYVVSVSS VYEQHESTPL
1351    RGRQKTGLDS PTGIDFSDIT ANSFTVHWIA PRATITGYRI RHHPEHFSGR
1401    PREDRVPHSR NSITLTNLTP GTEYVVSIVA LNGREESPLL IGQQSTVSDV
1451    PRDLEVVAAT PTSLLISWDA PAVTVRYYRI TYGETGGNSP VQEFTVPGSK
1501    STATISGLKP GVDYTITVYA VTGRGDSPAS SKPISINYRT EIDKPSQMQV
1551    TDVQDNSISV KWLPSSSPVT GYRVTTTPKN GPGPTKTKTA GPDQTEMTIE
1601    GLQPTVEYVV SVYAQNPSGE SQPLVQTAVT NIDRPKGLAF TDVDVDSIKI
1651    AWESPQGQVS RYRVTYSSPE DGIHELFPAP DGEEDTAELQ GLRPGSEYTV
1701    SVVALHDDME SQPLIGTQST AIPAPTDLKF TQVTPTSLSA QWTPPNVQLT
1751    GYRVRVTPKE KTGPMKEINL APDSSSVVVS GLMVATKYEV SVYALKDTLT
1801    SRPAQGVVTT LENVSPPRRA RVTDATETTI TISWRTKTET ITGFQVDAVP
1851    ANGQTPIQRT IKPDVRSYTI TGLQPGTDYK IYLYTLNDNA RSSPVVIDAS
1901    TAIDAPSNLR FLATTPNSLL VSWQPPRARI TGYIIKYEKP GSPPREVVPR
1951    PRPGVTEATI TGLEPGTEYT IYVIALKNNQ KSEPLIGRKK TDELPQLVTL
2001    PHPNLHGPEI LDVPSTVQKT PFVTHPGYDT GNGIQLPGTS GQQPSVGQQM
2051    IFEEHGFRRT TPPTTATPIR HRPRPYPPNV GEEIQIGHIP REDVDYHLYP
2101    HGPGLNPNAS TGQEALSQTT ISWAPFQDTS EYIISCHPVG TDEEPLQFRV
2151    PGTSTSATLT GLTRGATYNI IVEALKDQQR HKVREEVVTV GNSVNEGLNQ
2201    PTDDSCFDPY TVSHYAVGDE WERMSESGFK LLCQCLGFGS GHFRCDSSRW
2251    CHDNGVNYKI GEKWDRQGEN GQMMSCTCLG NGKGEFKCDP HEATCYDDGK
2301    TYHVGEQWQK EYLGAICSCT CFGGQRGWRC DNCRRPGGEP SPEGTTGQSY
2351    NQYSQRYHQR TNTNVNCPIE CFMPLDVQAD REDSRE
```

Matched peptides shown in **Bold Red**

Fig. S2. Peptide hits in the FN1 sequence indicated in red.

Hindawi Publishing Corporation
International Journal of Proteomics
Volume 2012, Article ID 897412, 10 pages
doi:10.1155/2012/897412

Review Article

Biomarker Discovery of Pancreatic and Gastrointestinal Cancer by 2DICAL: 2-Dimensional Image-Converted Analysis of Liquid Chromatography and Mass Spectrometry

Masaya Ono,[1] Masahiro Kamita,[1] Yusuke Murakoshi,[2] Junichi Matsubara,[3] Kazufumi Honda,[1] Banno Miho,[4] Tomohiro Sakuma,[4] and Tesshi Yamada[1]

[1] *Division of Chemotherapy and Clinical Research, National Cancer Center Research Institute, 5-1-1 Tsukiji, Chuo-ku, Tokyo 104-0045, Japan*
[2] *Third Department of Surgery, Tokyo Medical University, 6-7-1 Nishi-shinjuku, Shinjuku-ku, Tokyo 160-0023, Japan*
[3] *Institute for Stem Cell Biology and Regenerative Medicine (ISCBRM) and Stanford Cancer Center, Stanford University, 265 Campus Drive, Room G2015, Stanford, CA 94305, USA*
[4] *Bio Science Department, Research and Development Center, Mitsui Knowledge Industry Co., Ltd., 2-7-14 Higashinakano, Nakano-Ku, Tokyo 164-8555, Japan*

Correspondence should be addressed to Masaya Ono, masono@ncc.go.jp

Received 2 March 2012; Accepted 18 April 2012

Academic Editor: Fumio Nomura

Biomarkers tested by blood sample are of great use to clinicians as they provide useful information to aid an early and accurate diagnosis. Comprehensive "omics" studies are expected to facilitate the identification of such new biomarkers, and much research is being performed in this area. Our proteomics analysis system of 2-dimensional image-converted analysis of liquid chromatography and mass spectrometry (2DICAL) has successfully identified several new blood biomarkers from the clinical blood samples of pancreatic and colorectal cancer patients.

1. Introduction

Proteomic studies are powerful tools for identifying useful new biomarkers, and much research is currently being performed in this area. However, the blood proteome is extraordinary difficult to analyze because protein concentrations can vary by 12 orders of magnitude [1]. Thus, biomarker discovery using proteomics requires the development of effective pretreatment protocols to reduce the complexity of blood samples. The identification of biomarkers from clinical samples generally needs large numbers of samples to be compared. The same is true for the identification of biomarkers by mass-spectrometry-coupled proteomics [2, 3]. Our proteomics analysis system of 2-dimensional image-converted analysis of liquid chromatography and mass spectrometry (LC/MS; 2DICAL) and the procedure for reducing blood sample complexity have overcome these problems. We report the successful discovery of several new blood biomarkers for pancreatic and colorectal cancer [4, 5].

2. Biomarker Detection

2.1. Recruitment of Clinical Samples. For biomarker discovery, it is important to collect quality-controlled blood samples. We developed a multi-institutional protocol to preserve blood condition during sampling, storing, freezing, and thawing; all samples were collected and managed at the National Cancer Center Research Institute [6].

2.2. Sample Preparation. As the concentrations of different blood proteins can vary by over 12-orders of magnitude, it is essential to remove abundant proteins or to concentrate specific proteins before proteomics analysis. For this purpose, we used lectin affinity column [5, 7], major protein removal column [8], and hollow fiber membrane (HFM) [9, 10].

2.3. Biomarker Discovery. To identify candidate biomarkers from the proteomics data, we utilized our 2DICAL analysis

system that performs a quantitative comparison of unlabeled shotgun proteomics data generated by LC/MS and enables biomarker discovery from a large number of clinical samples. For selecting blood biomarkers, several decades of samples from cancer patients and healthy controls were analyzed by 2DICAL.

2.4. Biomarker Verification. Biomarkers selected by 2DICAL must be verified. As a rule, we first confirmed 2DICAL results using specific antibodies in small-scale immunoblotting assays. Once marker expression was detected and differences in the expression between patient and control samples were confirmed, large-scale verification was conducted. For this purpose, we used in-house reverse phase protein microarrays (RPPA), which can simultaneously assess hundreds of blood samples by antibody staining [11, 12]. Validation at the hundred-sample scale by multiple reaction monitoring/selective reaction monitoring (MRM/SRM) [13] is also ongoing.

3. Novel Applications of Analysis

We developed our original application for biomarker identification, that is, 2DICAL and RPPA.

3.1. 2DICAL. 2DICAL was developed as a shotgun proteomics analysis system. It analyzes the data of mass to charge ratio (m/z), peak intensity, retention time (RT), and each sample generated by LC/MS as the elemental data; it deploys various 2-dimensional images with different combinations of axes using these four elements. From the m/z-RT image, peaks derived from the same peptide in the direction of acquiring time are integrated. By adding algorisms to ensure reproducibility of m/z and RT, the same peak can be compared precisely across different samples, and a statistical comparison of identical peaks in different samples leads to the discovery of specific differentially expressed peptide peaks. Specific peaks are designated by their m/z and RT coordinates, and further analysis is based on these identifiers. Isotopic labeling is not necessary, and large numbers of samples can be analyzed in this way [4, 8].

3.2. RPPA. RPPA is an emerging high-throughput proteomics technique for validating new biomarkers [14, 15]. Furthermore, RPPA requires significantly lower amounts of clinical samples for quantification than established clinical tests such as enzyme-linked immunosorbent assay (ELISA). We made in-house RPPA using ProteoChip glass slides (Proteogen, Seoul, Republic of Korea) to test hundreds of blood samples simultaneously. For this technique, serially diluted samples are randomly plotted in quadruplicate in a 6,144-spot/slide format using a robot. The spotted slides are incubated with the primary antibody and biotinylated secondary antibody and then processed with a streptavidin-horseradish peroxidase conjugate. The stained slides are scanned on a microarray scanner. Statistical evaluation of the fluorescence intensity of individual samples is performed for large-scale validation of biomarker candidates [11, 12].

4. Biomarkers for Pancreatic Cancer and Gastrointestinal Cancer

Several blood biomarkers have already been discovered. Sample recruitment, sample preparation, biomarker discovery, and validation have been described for each biomarker.

4.1. Biomarkers for Pancreatic Cancer. Prolyl-hydroxylated α-fibrinogen [5] and CXC chemokine ligand 7 (CXCL-7) [10] were identified as pancreatic cancer biomarkers.

4.1.1. Prolyl-Hydroxylated α-Fibrinogen

Objective. Screening for pancreatic cancer.

Samples. In total, 86 plasma samples (collected from 43 patients with pancreatic ductal adenocarcinomas and 43 healthy controls) were used for biomarker identification, and 273 plasma samples (collected from 160 patients with pancreatic ductal adenocarcinomas and 113 healthy controls) were used for validation.

Sample Preparation. Samples were treated with concanavalin A (Con A) to reduce plasma protein complexity.

Biomarker Discovery. Samples were subjected to LC/MS and analyzed by 2DICAL. A total of 115325 peaks were detected, and 6 peaks of 412 m/z (RT 13.7 min), 546 m/z (8.3 min), 552 m/z (8.3 min), 827 m/z (8.3 min), 1141 m/z (29.0 min), and 1185 m/z (9.2 min) were statistically significant with >2 fold difference and $P < 0.0005$ (Mann-Whitney U test) between the pancreatic cancer patient group and healthy control group. Three of the 6 peaks were identified as hydroxyproline-modified α-fibrinogen fragments (Figure 1(a)).

Biomarker Validation. An antibody recognizing α-fibrinogen fragments with an ESSSHH P*GIAEFPSR (P*, 4-hydroxyproline) modification was generated and used for small-scale confirmation of the expression of prolyl-hydroxylated α-fibrinogen and the differences in the expression of modified protein between samples of pancreatic cancer patients and healthy controls (Figure 1(b)). A competitive ELISA was developed using this antibody to quantify plasma levels of prolyl-hydroxylated α-fibrinogen. A significant difference in prolyl-hydroxylated α-fibrinogen expression between plasma samples from pancreatic cancer patients and healthy controls was observed ($P = 3.80 \times 10^{-15}$, Mann-Whitney U test; Figure 1(c)).

4.1.2. CXCL-7

Objective. Screening for pancreatic cancer.

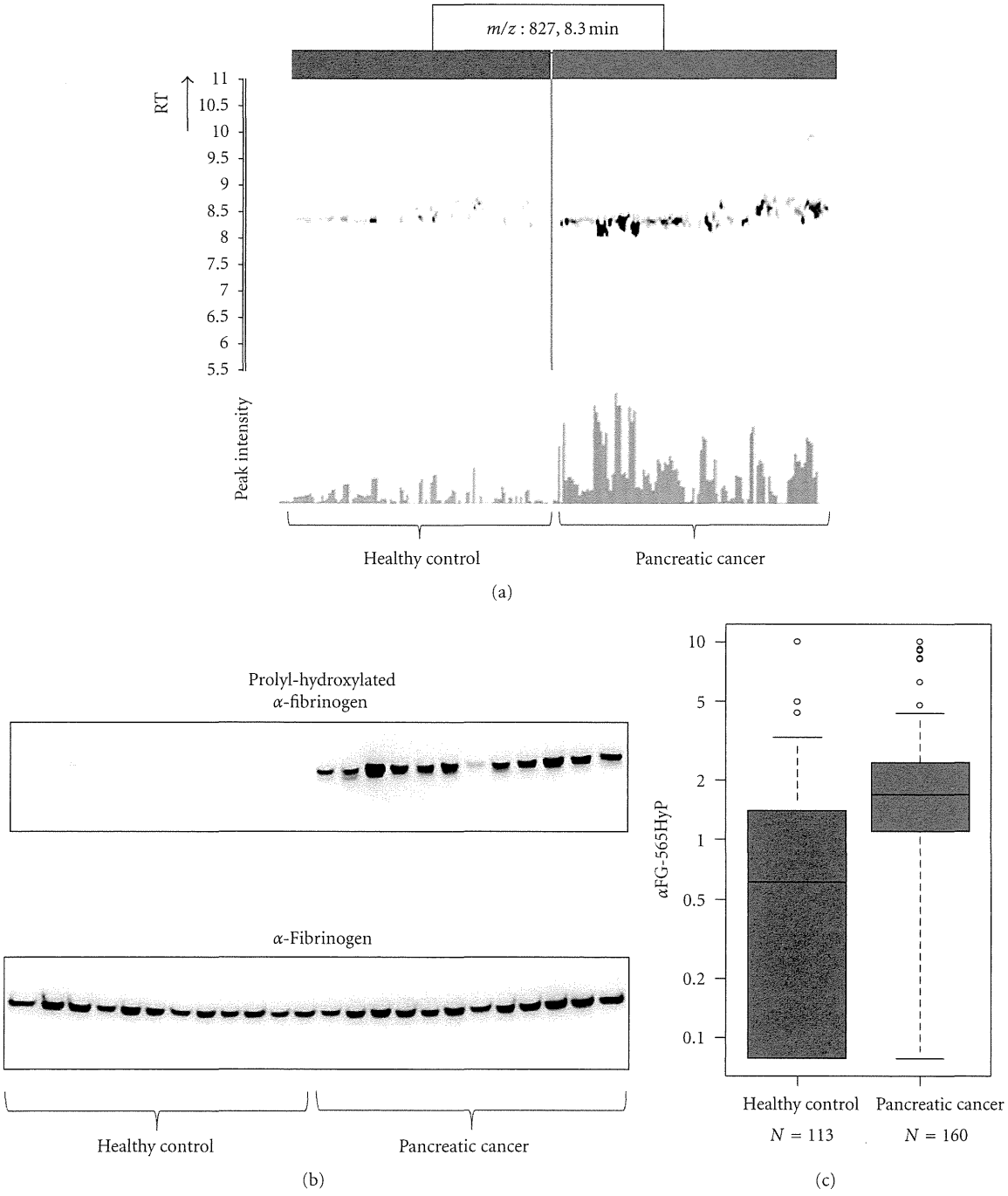

FIGURE 1: Discovery and validation of prolyl-hydroxylated α-fibrinogen as a pancreatic cancer biomarker (partially changed from [5]). (a) 2DICAL images of the peak (*m/z*, 827; RT, 8.3 min) with coordinates RT versus patients (upper) and intensity versus patients (lower). Red indicates samples from pancreatic cancer patients, and blue indicates samples from healthy controls. (b) Western blot of prolyl-hydroxylated α-fibrinogen (upper panel) and total α-fibrinogen (lower panel). (c) Large-scale ELISA validation of the plasma level of prolyl-hydroxylated α-fibrinogen using hundreds of clinical samples.

Samples. A total of 45 plasma samples (collected from 24 patients with pancreatic ductal adenocarcinomas and 21 healthy controls) were used for biomarker discovery and 227 plasma samples (collected from 140 patients with pancreatic ductal adenocarcinomas and 87 healthy controls) were used for biomarker validation.

Sample Preparation. Samples were treated with HFM to reduce plasma protein complexity.

Biomarker Discovery. Samples were subjected to LC/MS and analyzed by 2DICAL. A total of 53009 peaks were detected, and 140 peaks were differentially expressed between

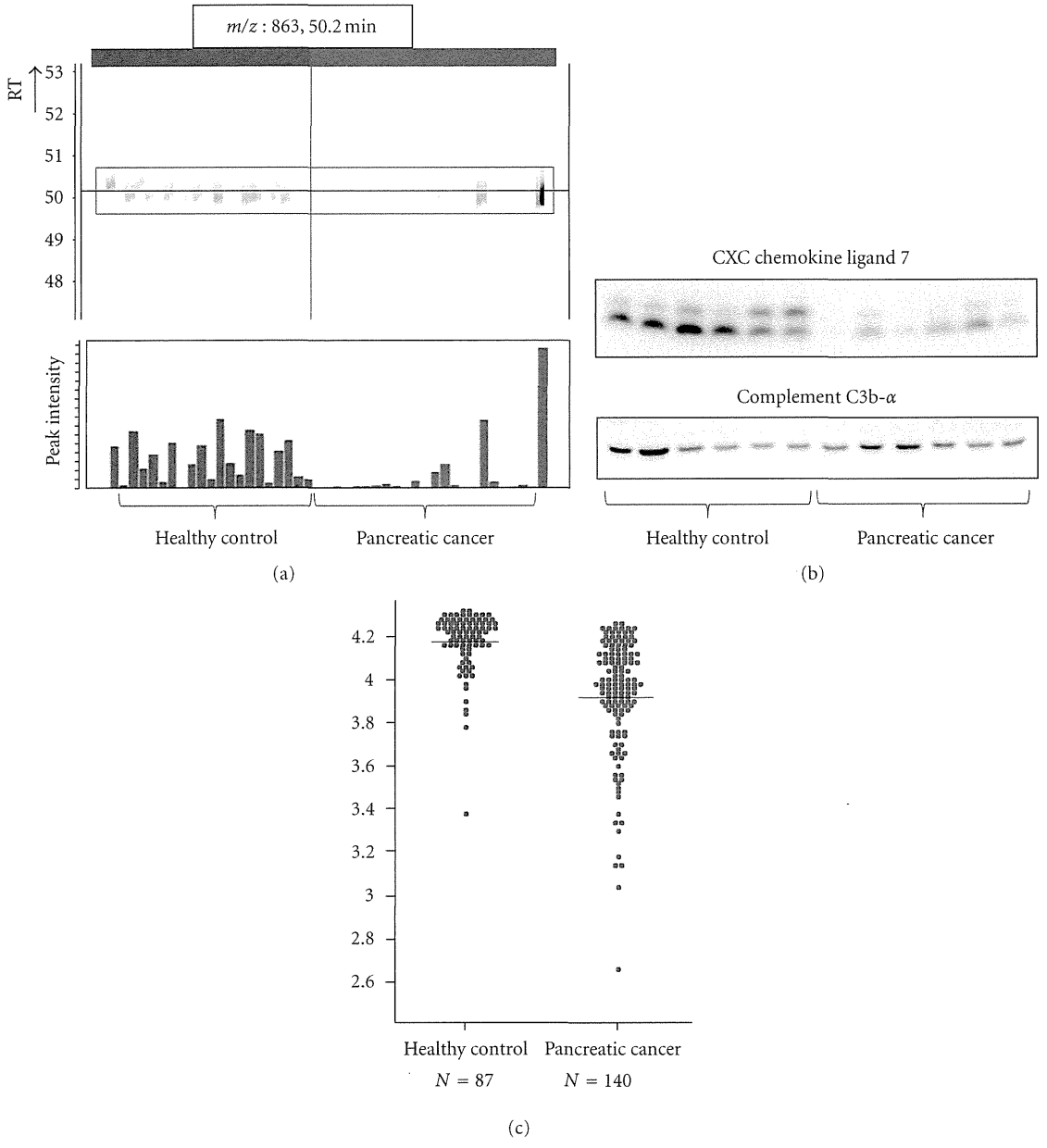

FIGURE 2: Discovery and validation of CXC chemokine ligand 7 as a pancreatic cancer biomarker (partially changed from [10]). (a) 2DICAL images of peptide peak (*m/z*, 863; RT, 50.2 min) with coordinates RT versus patients (upper) and intensity versus patients (bottom). Red indicates samples from pancreatic cancer patients, and blue indicates samples from healthy controls. (b) Western blot of CXC chemokine ligand 7 (upper panel) and the loading control Complement C3b-α. (c) Large-scale RPPA validation of the plasma level of CXC chemokine ligand 7 using hundreds of clinical samples.

pancreatic cancer patients and healthy controls, with an area under curve (AUC) of >0.800. Of these, 10 proteins were annotated by database search of tandem mass spectra. The 862 *m/z* (RT 50.2 min) peak annotated as a fragment of CXCL-7 was specifically expressed in pancreatic cancer patients, with an AUC of 0.839 ($P = 4.54 \times 10^{-5}$ by Mann-Whitney U test) (Figure 2(a)).

Biomarker Validation. Small-scale confirmation of CXCL7 identification and differential expression was done by immunoblotting using an anti-CXCL-7 antibody (Figure 2(b)). For large-scale validation, 227 plasma samples were randomly plotted onto ProteoChip glass slides for RPPA and blotted with an anti-CXCL-7 antibody. CXCL7 expression in pancreatic cancer patients and healthy controls was confirmed to be significantly different ($P = 1.40 \times 10^{-16}$, Welch t-test; Figure 2(c)).

4.2. Biomarkers for Colorectal Cancer. Complement Component 9 (C9) [12] and adipophilin [16] were identified as colorectal cancer biomarkers.

4.2.1. C9

Objective. Screening for colorectal cancer.

Samples. In total, 90 plasma samples (collected from 31 colorectal cancer patients and 59 healthy controls) were used for biomarker discovery, and 345 plasma samples (collected from 115 colorectal cancer patients and 230 healthy controls) were used for validation.

Sample Preparation. Samples were treated with a 12-abundant-plasma-protein removal columns to reduce plasma protein complexity.

Biomarker Discovery. Samples were subjected to LC/MS and analyzed by 2DICAL. A total of 94803 peaks were detected, and 90 peaks showed statistically significant differences in expression between plasma from colorectal cancer patients and healthy controls. Of these, 10 proteins were annotated by database search of tandem mass spectra. A peptide peak with 622 m/z (RT 56.8 min) was annotated as a fragment of C9 specific to colorectal cancer patients ($P = 3.0 \times 10^{-5}$, paired t-test; Figure 3(a)).

Biomarker Validation. Small-scale confirmation of C9 identification and differential expression was done by immunoblotting using an anti-C9 antibody (Figure 3(b)). For large-scale validation, 345 plasma samples were randomly plotted into ProteoChip glass slides for RPPA and blotted with an anti-C9 antibody. There was a significant difference in C9 expression in plasma from colorectal cancer patients and from healthy controls ($P = 1.43 \times 10^{-12}$, Student's t-test; Figure 3(c)).

4.2.2. Adipophilin

Objective. Screening for colorectal cancer.

Samples. A total of 43 plasma samples (collected from 22 colorectal cancer patients and 21 healthy controls) were used for biomarker discovery, and 323 plasma samples (collected from 127 colorectal cancer patients and 196 healthy controls) were used for validation.

Sample Preparation. Samples were treated with HFM to reduce plasma protein complexity.

Biomarker Discovery. Pretreated samples were subjected to LC/MS and analyzed by 2DICAL. A total of 53009 peptide peaks were detected, and 103 peaks with an AUC of >0.800 were differentially expressed in healthy controls and colorectal cancer patients. Of these, 6 proteins were annotated by database search of tandem mass spectra. The 749 m/z (RT 47.4 min) peak represents a fragment of adipophilin specifically present in colorectal cancer patients (0.814 in AUC; Figure 4(a)).

Biomarker Validation. Small-scale confirmation of adipophilin identification and differential expression was done by immunoblotting using an anti-adipophilin antibody (Figure 4(b)). For large-scale validation, 323 plasma samples were randomly plotted into ProteoChip glass slides for RPPA and blotted with an anti-adipophilin antibody. Differential expression of adipophilin between plasma samples from colorectal cancer patients and from healthy controls was significant ($P = 5.49 \times 10^{-10}$, Welch t-test; Figure 4(c)).

4.3. Biomarker for Adverse Effects in Pancreatic Cancer following Chemotherapy

4.3.1. Haptoglobin [17]

Objective. Prediction for the adverse effect of pancreatic cancer chemotherapy.

Samples. A total of 47 plasma samples collected from patients with pancreatic ductal adenocarcinomas and treated with gemcitabine (2′,2′-difluorodeoxycytidine) monotherapy (25 with severe adverse effects (AEs) and 22 without) were used for biomarker discovery, and 253 plasma samples and 52 serum samples were collected from patients with pancreatic ductal adenocarcinomas treated by gemcitabine monotherapy for validation.

Sample Preparation. Samples were treated with a 12 abundant plasma protein removal column to reduce plasma protein complexity.

Biomarker Discovery. Samples were subjected to LC/MS and analyzed by 2DICAL. A total of 60,888 peaks were detected and 757 peaks differed significantly between patients with severe AEs and patients without AEs ($P < 0.001$, Welch t-test). Among these, the peak with highest value to discriminate patients with severe AEs from those without AEs was annotated as haptoglobin. The haptoglobin fragment peak of 491 m/z (RT 44.5 min) is shown in Figure 5(a).

Biomarker Validation. Small-scale confirmation of haptoglobin identification and differential expression was confirmed by immunoblotting using an anti-haptoglobin antibody (Figure 5(b)). Haptoglobin concentration in 305 plasma and serum samples was measured by immunonephelometry. The severity of AE severity inversely correlated with the concentration of haptoglobin (Figure 5(c)).

4.4. Biomarker for Predicting Survival of Pancreatic Cancer Patients following Chemotherapy

4.4.1. α1-Antitrypsin [11]

Objective. Prediction of the survival for pancreatic cancer chemotherapy.

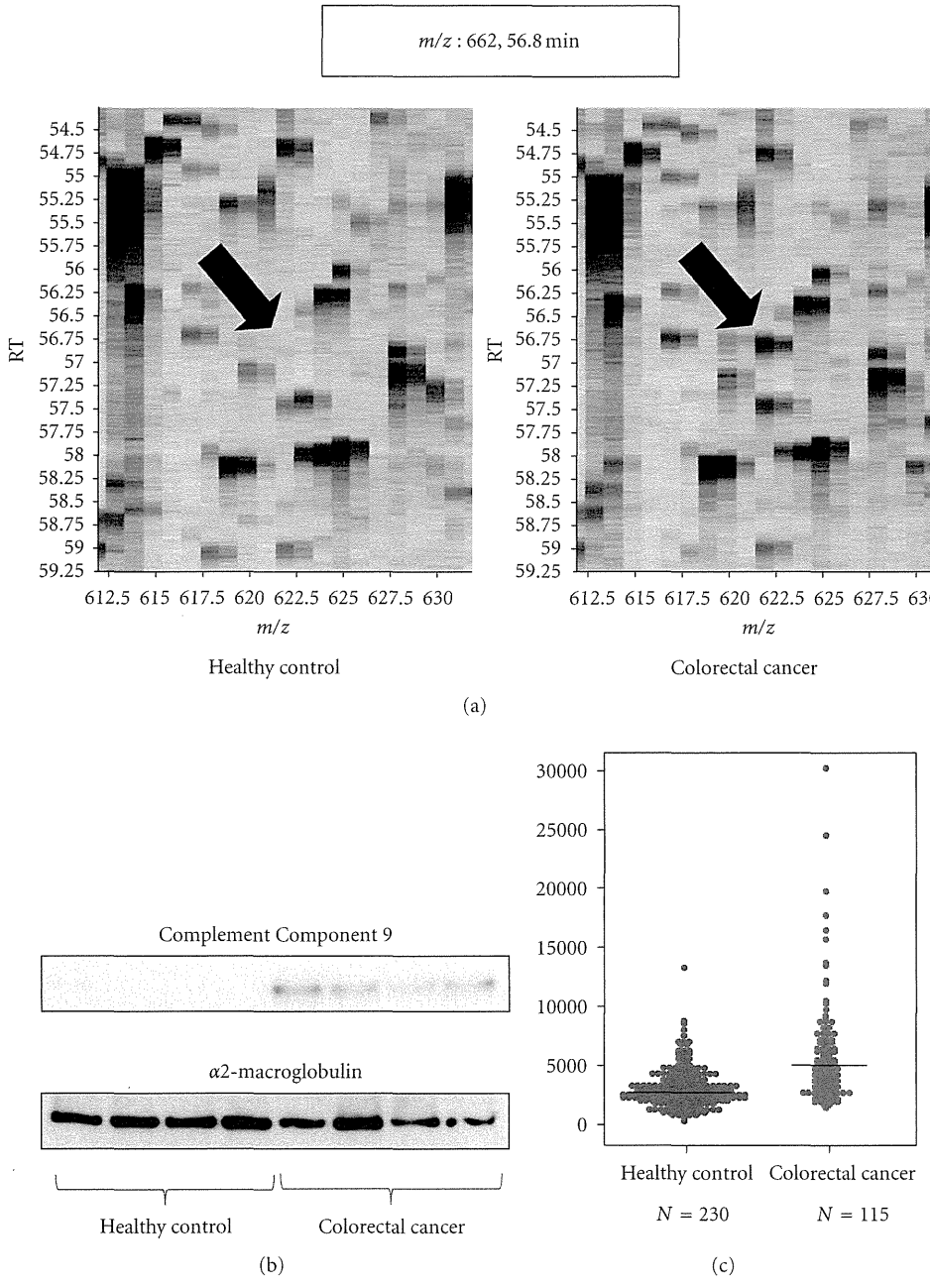

FIGURE 3: Discovery and validation of Complement Component 9 as a colorectal cancer biomarker (partially changed from [12]). (a) 2DICAL images with coordinates *m/z* versus RT. The intensity of the peak of 622 *m/z* and RT of 56.8 min (indicated by arrows) are clearly different in the plasma samples from healthy controls (left) and colorectal cancer patients (right). (b) Western blot of Complement Component 9 and the loading control α2-macroglobulin. (c) Large-scale RPPA validation of the plasma level of Complement Component 9 using hundreds of clinical samples.

Samples. A total of 60 plasma samples collected from patients with pancreatic ductal adenocarcinomas and treated by gemcitabine monotherapy (29 with short-term survival and 31 with long-term survival) were used for biomarker discovery, and 304 samples collected from patients with pancreatic ductal adenocarcinomas and treated by gemcitabine monotherapy were used for validation.

Sample Preparation. Samples were treated with 12-abundant-plasma-protein removal column to reduce plasma protein complexity.

Biomarker Discovery. Samples were subjected to LC/MS and analyzed by 2DICAL. A total of 45227 peaks were detected, and 637 peaks differed significantly between patients with

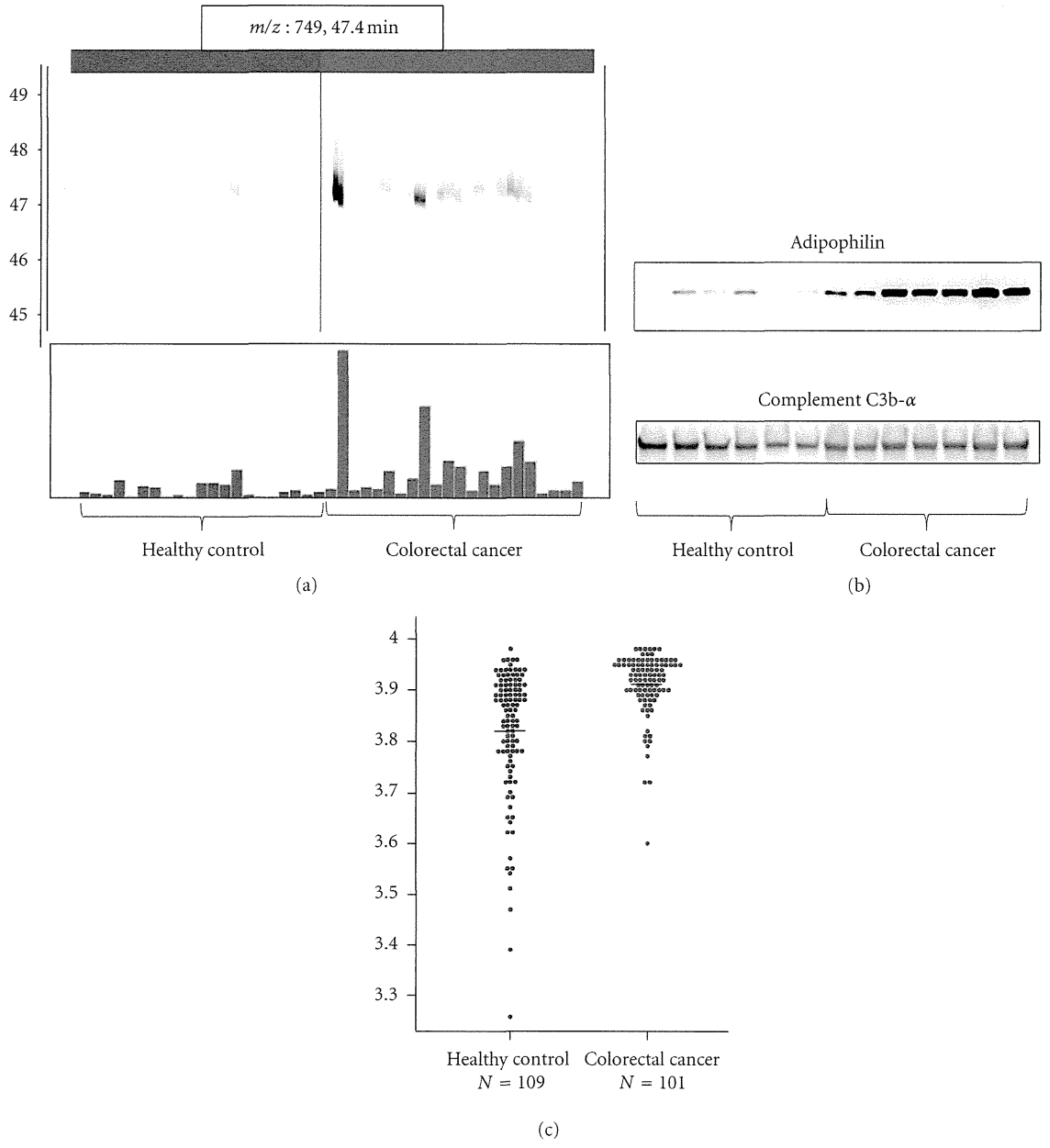

FIGURE 4: Discovery and validation of adipophilin as a colorectal cancer biomarker (partially changed from [16]). (a) 2DICAL images of the peak (*m/z*, 749; RT, 47.4 min) with coordinates RT versus patients (upper) and intensity versus patients (lower). Red indicates samples from colorectal cancer patients, and blue indicates samples from healthy controls. (b) Western blot of adipophilin and the loading control Complement C3b-α. (c) Large-scale RPPA validation of the plasma level of adipophilin using hundreds of clinical samples.

long-term survival and those with short-term survival ($P < 0.001$, Welch t-test). The peptide peak that best discriminated patients with short-term survival from those with long-term survival ($P = 2.57 \times 10^{-4}$) at 491 *m/z* (RT 44.5 min) was annotated as a fragment of a1-antitrypsin (Figure 6(a)).

Biomarker Validation. Small-scale confirmation of α1-antitrypsin identification and differential expression was done by immunoblotting using an anti-α1-antitrypsinantibody (Figure 6(b)). For large-scale validation, 304 samples were randomly plotted into ProteoChip glass slides for RPPA and blotted with antibody to α1-antitrypsin. Improved survival of patients with pancreatic ductal adenocarcinoma treated by gemcitabine monotherapy correlated with low blood concentrations of α1-antitrypsin (Figure 6(c)).

5. Conclusions

We have established a comprehensive method for identifying blood biomarkers, which covers all aspects of analysis from

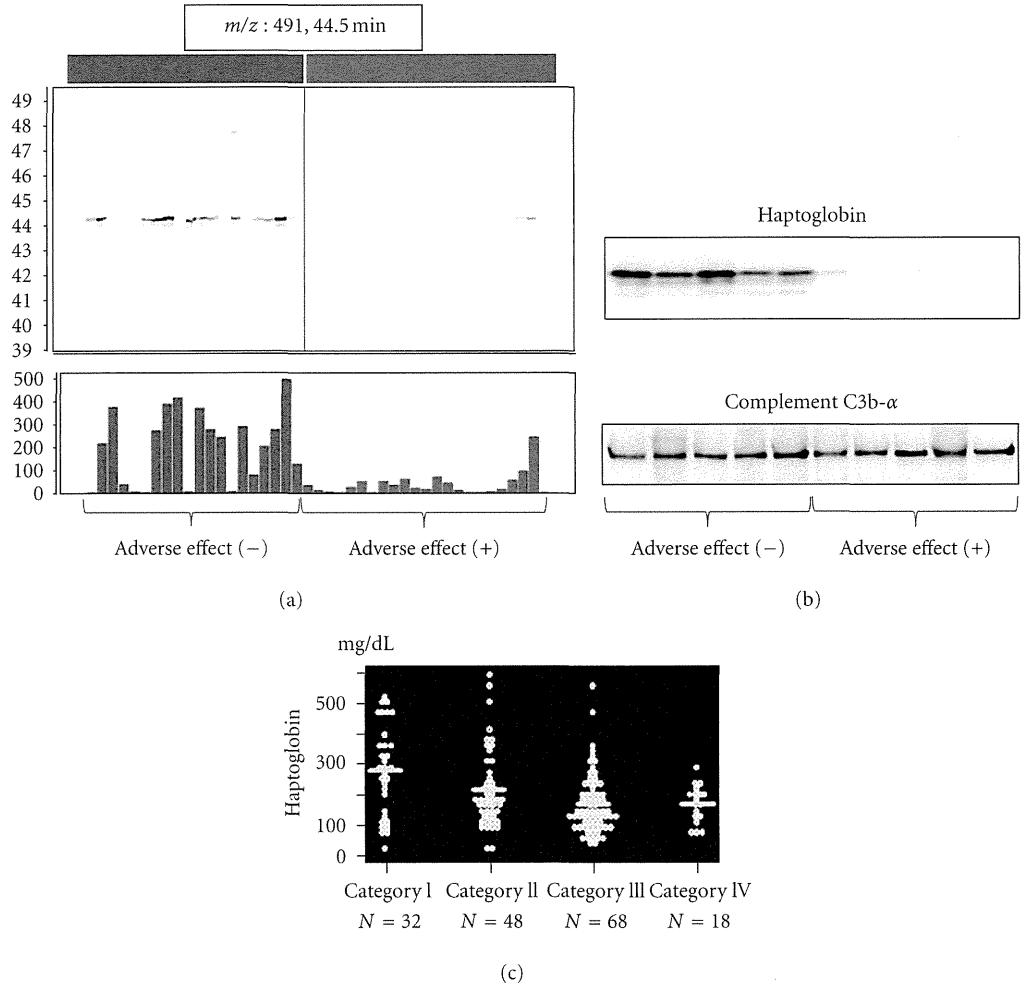

FIGURE 5: Discovery and validation of haptoglobin as a biomarker for adverse effects in pancreatic cancer following chemotherapy (partially changed from [17]). (a) 2DICAL images of the peak (m/z, 409; RT, 44.5 min) with coordinates RT versus patients (upper) and intensity versus patients (lower). Red indicates samples from pancreatic cancer patients with severe AEs following chemotherapy, and blue indicates samples from pancreatic cancer patients without AEs following chemotherapy. (b) Western blot of haptoglobin and the loading control Complement C3b-α. (c) Large-scale immunonephelometric validation of the plasma level of haptoglobin using hundreds of clinical samples. The adverse effects were categorized in four grades according to the degree of neutropenia and thrombocytopenia. Haptoglobin concentration decreased according to the increase of the adverse effect severity.

sample recruitment to biomarker discovery and validation. The next stage in the development of these novel biomarkers is to test them in a clinical context. The proteomics approach for blood biomarker discovery identifies a new function for common proteins such as these biomarkers. With technological advances in sample preparations, resolution and sensitivity of mass spectrometer, and methods for the identification of proteins from mass spectra, we can expect to discover biomarkers existing in much smaller amount or those with new structures in the future. We also expect that large-scale validation of biomarkers discovered using mass spectrometer will be conducted by MRM/SRM. 2DICAL is applicable not only for proteomics but also for metabolomics or glycomics and has a great potential for identifying disease-associated post-translational protein modifications. 2DICAL will evolve along with technological advances and contribute the discovery of new biomarkers in future.

Acknowledgments

The authors thank Ms. Ayako Ikarashi, Ms. Tomoko Umaki, and Ms. Yuka Nakamura for their technical assistance. Funding was provided by the Program for Promotion of Fundamental Studies in Health Sciences conducted by the National Institute of Biomedical Innovation of Japan, the Third-Term Comprehensive Control Research for Cancer and Research on Biological Markers for New Drug Development conducted by the Ministry of Health and Labor of Japan. These sponsors had no role in the design of the study, collection of the data, analysis and interpretation of the data, decision to submit the paper for publication, or writing of the paper.

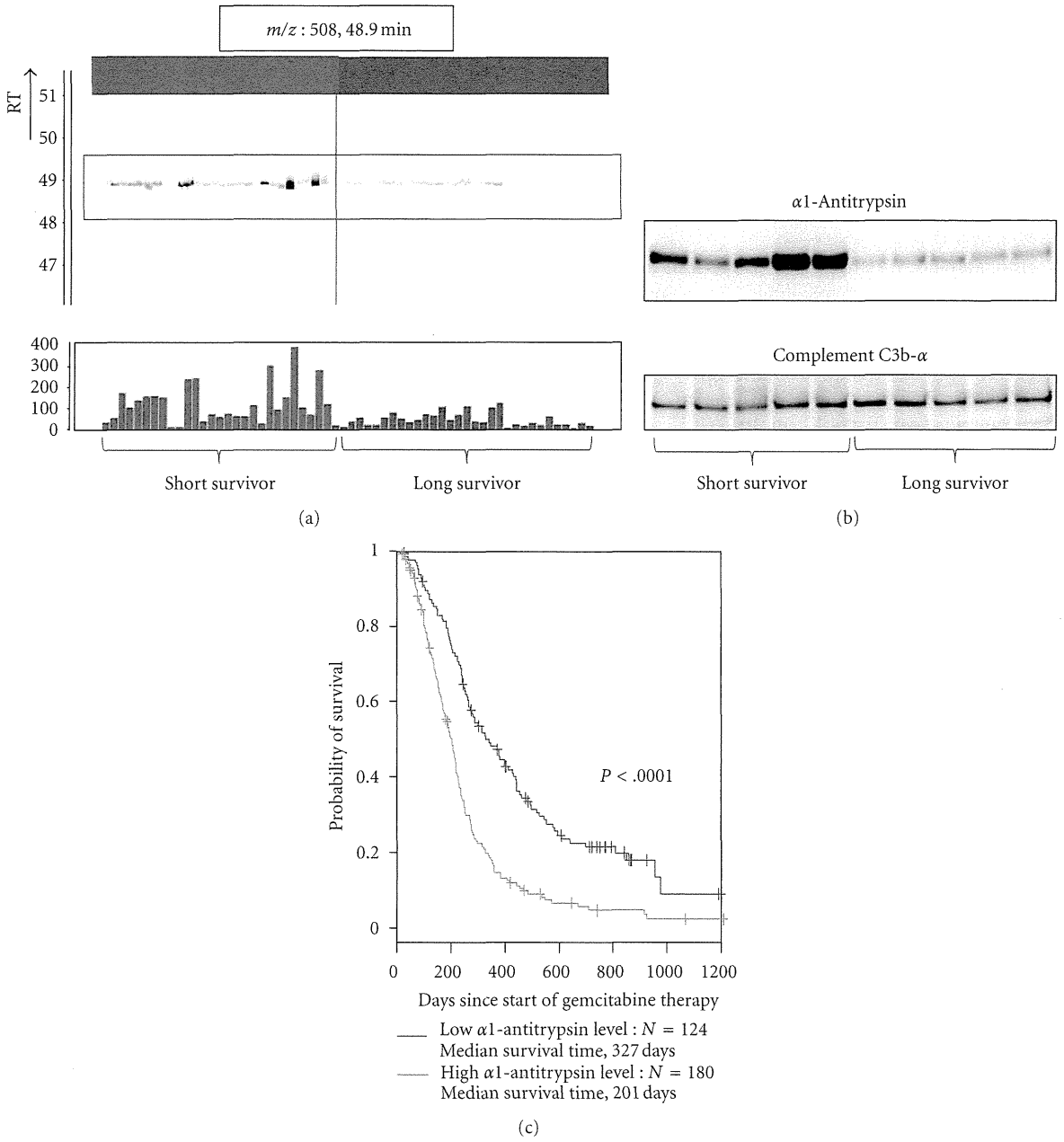

FIGURE 6: Discovery and validation of α1-antitrypsin as a biomarker for predicting survival of pancreatic cancer patients following chemotherapy (partially changed from [11]). (a) 2DICAL images of the peak (*m/z*, 508; RT, 48.9 min) with coordinates RT versus patients (upper) and intensity versus patients (lower). Red indicates samples from pancreatic cancer patients with short-term survival, and blue indicates samples from pancreatic cancer patients with long-term survival. (b) Western blot of α1-antitrypsin and the loading control Complement C3b-α. (c) Large-scale RPPA validation of the plasma level of α1-antitrypsin using hundreds of clinical samples. Survival curve was significantly better in the group of low α1-antitrypsin level than that of high α1-antitrypsin level.

References

[1] N. L. Anderson and N. G. Anderson, "The human plasma proteome: history, character, and diagnostic prospects," *Molecular & Cellular Proteomics*, vol. 1, no. 11, pp. 845–867, 2002.

[2] S. P. Gygi, B. Rist, S. A. Gerber, F. Turecek, M. H. Gelb, and R. Aebersold, "Quantitative analysis of complex protein mixtures using isotope-coded affinity tags," *Nature Biotechnology*, vol. 17, no. 10, pp. 994–999, 1999.

[3] L. DeSouza, G. Diehl, M. J. Rodrigues et al., "Search for cancer markers from endometrial tissues using differentially labeled tags iTRAQ and cICAT with multidimensional liquid chromatography and tandem mass spectrometry," *Journal of Proteome Research*, vol. 4, no. 2, pp. 377–386, 2005.

[4] M. Ono, M. Shitashige, K. Honda et al., "Label-free quantitative proteomics using large peptide data sets generated by nanoflow liquid chromatography and mass spectromery," *Molecular and Cellular Proteomics*, vol. 5, no. 7, pp. 1338–1347, 2006.

[5] M. Ono, J. Matsubara, K. Honda et al., "Prolyl 4-hydroxylation of α-fibrinogen. A novel protein modification revealed by

plasma proteomics," *Journal of Biological Chemistry*, vol. 284, no. 42, pp. 29041–29049, 2009.

[6] K. Honda, Y. Hayashida, T. Umaki et al., "Possible detection of pancreatic cancer by plasma protein profiling," *Cancer Research*, vol. 65, no. 22, pp. 10613–10622, 2005.

[7] S. Ogata, T. Muramatsu, and A. Kobata, "Fractionation of glycopeptides by affinity column chromatography on concanavalin A Sepharose," *Journal of Biochemistry*, vol. 78, no. 4, pp. 687–696, 1975.

[8] A. Negishi, M. Ono, Y. Handa et al., "Large-scale quantitative clinical proteomics by label-free liquid chromatography and mass spectrometry," *Cancer Science*, vol. 100, no. 3, pp. 514–519, 2009.

[9] Y. Tanaka, H. Akiyama, T. Kuroda et al., "A novel approach and protocol for discovering extremely low-abundance proteins in serum," *Proteomics*, vol. 6, no. 17, pp. 4845–4855, 2006.

[10] J. Matsubara, K. Honda, M. Ono et al., "Reduced plasma level of CXC chemokine ligand 7 in patients with pancreatic cancer," *Cancer Epidemiology Biomarkers and Prevention*, vol. 20, no. 1, pp. 160–171, 2011.

[11] J. Matsubara, M. Ono, K. Honda et al., "Survival prediction for pancreatic cancer patients receiving gemcitabine treatment," *Molecular and Cellular Proteomics*, vol. 9, no. 4, pp. 695–704, 2010.

[12] Y. Murakoshi, K. Honda, S. Sasazuki et al., "Plasma biomarker discovery and validation for colorectal cancer by quantitative shotgun mass spectrometry and protein microarray," *Cancer Science*, vol. 102, no. 3, pp. 630–638, 2011.

[13] E. M. H. Finlay, D. E. Games, J. R. Startin, and J. Gilbert, "Screening, confirmation, and quantification of sulphonamide residues in pig kidney by tandem mass spectrometry of crude extracts," *Biomedical and Environmental Mass Spectrometry*, vol. 13, no. 11, pp. 633–639, 1986.

[14] T. Grote, D. R. Siwak, H. A. Fritsche et al., "Validation of reverse phase protein array for practical screening of potential biomarkers in serum and plasma: accurate detection of CA19-9 levels in pancreatic cancer," *Proteomics*, vol. 8, no. 15, pp. 3051–3060, 2008.

[15] J. D. Wulfkuhle, L. A. Liotta, and E. F. Petricoin, "Proteomic applications for the early detection of cancer," *Nature Reviews Cancer*, vol. 3, no. 4, pp. 267–275, 2003.

[16] J. Matsubara, K. Honda, M. Ono et al., "Identification of adipophilin as a potential plasma biomarker for colorectal cancer using label-free quantitative mass spectrometry and protein microarray," *Cancer Epidemiology, Biomarkers and Prevention*, vol. 20, no. 10, pp. 2195–2203, 2011.

[17] J. Matsubara, M. Ono, A. Negishi et al., "Identification of a predictive biomarker for hematologic toxicities of gemcitabine," *Journal of Clinical Oncology*, vol. 27, no. 13, pp. 2261–2268, 2009.

International Scholarly Research Network
ISRN Oncology
Volume 2012, Article ID 768190, 10 pages
doi:10.5402/2012/768190

Clinical Study

Carbonic Anhydrase I as a New Plasma Biomarker for Prostate Cancer

Michiko Takakura,[1] Akira Yokomizo,[2] Yoshinori Tanaka,[3] Michimoto Kobayashi,[3] Giman Jung,[3] Miho Banno,[4] Tomohiro Sakuma,[4] Kenjiro Imada,[2,5] Yoshinao Oda,[5] Masahiro Kamita,[1] Kazufumi Honda,[1] Tesshi Yamada,[1] Seiji Naito,[2] and Masaya Ono[1]

[1] *Division of Chemotherapy and Clinical Research, National Cancer Center Research Institute, 5-1-1 Tsukiji, Chuo-ku, Tokyo 104-0045, Japan*
[2] *Department of Urology, Graduate School of Medical Sciences, Kyushu University, 3-1-1 Maidashi, Higashi-ku, Fukuoka 812-8582, Japan*
[3] *New Frontiers Research Laboratories, Toray Industries, Inc., 10-1 Tebiro, Kanagawa, Kamakura 248-8555, Japan*
[4] *Bio Science Department, Research and Development Center, Mitsui Knowledge Industry Co., Ltd., 2-7-14 Higashinakano, Nakano-Ku, Tokyo 164-8555, Japan*
[5] *Department of Anatomic Pathology, Graduate School of Medical Sciences, Kyushu University, 3-1-1 Maidashi, Higashi-ku, Fukuoka 812-8582, Japan*

Correspondence should be addressed to Masaya Ono, masono@ncc.go.jp

Received 17 September 2012; Accepted 2 October 2012

Academic Editors: A. E. Bilsland, B. Comin-Anduix, G. Ferrandina, and S. Holdenrieder

Serum prostate-specific antigen (PSA) levels ranging from 4 to 10 ng/mL is considered a diagnostic gray zone for detecting prostate cancer because biopsies reveal no evidence of cancer in 75% of these subjects. Our goal was to discover a new highly specific biomarker for prostate cancer by analyzing plasma proteins using a proteomic technique. Enriched plasma proteins from 25 prostate cancer patients and 15 healthy controls were analyzed using a label-free quantitative shotgun proteomics platform called 2DICAL (2-dimensional image converted analysis of liquid chromatography and mass spectrometry) and candidate biomarkers were searched. Among the 40,678 identified mass spectrum (MS) peaks, 117 peaks significantly differed between prostate cancer patients and healthy controls. Ten peaks matched carbonic anhydrase I (CAI) by tandem MS. Independent immunological assays revealed that plasma CAI levels in 54 prostate cancer patients were significantly higher than those in 60 healthy controls ($P = 0.022$, Mann-Whitney U test). In the PSA gray-zone group, the discrimination rate of prostate cancer patients increased by considering plasma CAI levels. CAI can potentially serve as a valuable plasma biomarker and the combination of PSA and CAI may have great advantages for diagnosing prostate cancer in patients with gray-zone PSA level.

1. Introduction

Prostate cancer is the most common malignancy in the United State. In 2009, 192,280 men were estimated to have been diagnosed with prostate cancer, and 27,360 of these patients died in the United States [1]. The prostate-specific antigen (PSA) is used for the detection of prostate cancer in daily practice, but its diagnostic reliability is hampered by its low specificity. Thus, serum PSA levels ranging from 4 to 10 ng/mL are called the "gray zone" in which it is very difficult to discriminate between patients with prostate cancer and those with benign prostatic hyperplasia (BPH), prostatitis, or normal prostate. Furthermore, among the patients with serum PSA levels between 4 to 10 ng/mL, only 25% will be found to have prostate cancer [2]. Serum PSA levels can also increase in prostatitis, [3, 4] and approximately 20%–30% of prostate cancers are missed when the cut-off value is set to 4 ng/mL [5–7]. The false negative rate in the first biopsy is estimated between 12% and 32% [8, 9], and a large population of men with chronically high serum PSA

levels undergo repeated biopsies to eliminate the possibility of prostate cancer [3, 4].

Our quantitative label-free shotgun proteomics analysis system, called 2-dimensional image converted analysis of liquid chromatography and mass spectrometry (2DICAL), can accurately align different liquid chromatography-mass spectrometry (LC-MS) data sets, enabling rapid comparison of a statistically sufficient number of clinical samples [10–16]. 2DICAL has a characteristic of top-down proteomics in shotgun proteomics. It converts the LC-MS spectrum data into peaks on a 2-dimensional plane with axes of mass-to-charge ratio (m/z) and retention time (RT). The peaks with the same m/z and RT are compared across the samples, and statistically significant peaks are selected. Targeted tandem mass spectrometry (MS) is conducted on the selected peaks, and the peaks are annotated by sequence search programs (see Supplemental Materials available online at doi: 10.5402/2012/768190).

Here we describe the discovery of a new candidate biomarker for prostate cancer diagnosis that we uncovered using 2DICAL to compare the plasma proteomes of prostate cancer patients with those of healthy controls.

2. Materials and Methods

2.1. Clinical Samples. Plasma samples were prospectively collected at the Department of Urology and Ophthalmology, Graduate School of Medical Sciences, Kyushu University (Fukuoka, Japan), between October 2000 and January 2008 from 162 individuals, including those suffering from prostate cancer ($n = 54$), renal cell cancer (RCC; $n = 20$), prostatitis ($n = 6$), and BPH ($n = 22$) and 60 healthy individuals who had no symptom and PSA below 10 ng/mL, and those with PSA over 4 ng/mL were periodically followed in outpatient clinic with no evidence of prostate cancer. Prostate cancer patients were definitively diagnosed by prostate biopsy. Patient characteristics including age, PSA levels, Gleason score, and TNM classification are shown in Table 1. For 2DICAL analysis, we selected prostate cancer patients and age-matched healthy controls. All patients provided written informed consent authorizing the collection and use of their samples for research. The institutional ethics committee boards of the National Cancer Center Research Institute (Tokyo, Japan) and the Kyushu University reviewed and approved our protocol.

2.2. Sample Preparation. To exclude sampling bias, 7 mL of each patient's whole blood was collected in a tube containing ethylenediaminetetraacetic acid-2Na (Venoject II, Terumo, Japan) before surgery or first treatment. Plasma was prepared by centrifuging samples at 1,050 ×g for 10 min at 4°C. Aliquots of 1 mL were added to 1.5-mL Eppendorf tubes and frozen at −80°C until analysis. Control samples were collected and stored identically. All samples were subjected to only 1 freeze-thaw cycle. To enrich low molecular weight plasma proteins, 500 μL of plasma was diluted to 4 mL by adding 25 mM ammonium bicarbonate buffer (pH 8.0), and the diluted plasma samples were processed using a hollow fiber membrane-based low molecular weight (LMW) protein enrichment device as described previously [14, 17]. The device employs multistage filtration and cascaded cross-flow processes, and the proteins smaller than a predetermined molecular weight can be separated in a fully automated operation. The solution enriched for LMW proteins was recovered for 1 h operation and the LMW proteins were digested at 37°C for 18 h with sequencing grade modified trypsin (Promega, Madison, WI).

2.3. LC-MS. Trypsin-digested samples were analyzed in duplicate by nanoflow high-performance liquid chromatography (NanoFrontier nLC, Hitachi High-technologies, Tokyo, Japan) connected to an electrospray ionization quadrupole time-of-flight mass spectrometer (Q-Tof Ultima, Waters, Milford, MA). MS peaks were detected, normalized, and quantified using our 2DICAL software package [10, 12]. A serial identification (ID) number was applied to each of the MS peaks detected. The reproduction of LC-MS was monitored by calculating the correlation coefficient (CC) and coefficient of variance (CV) of every measurement.

2.4. Protein Identification by Tandem Mass Spectrometry (MS/MS). Peak lists were generated using the Mass Navigator software package (Mitsui Knowledge Industry, Tokyo, Japan) and searched against the SwissProt database using the Mascot software package (Matrix Science, London, UK). Search parameters used were as follows: human protein sequences were selected, trypsin was designated as the enzyme, and up to 1 missed cleavage was allowed. Mass tolerances for precursor and fragment ions were ±0.6 Da and ±0.2 Da, respectively. The score threshold was set to a Mascot score >30. If a peptide matched to multiple proteins, the protein name with the highest Mascot score was selected.

2.5. Western Blot Analysis. Plasma samples were analyzed by sodium dodecyl sulfate-polyacrylamide gel electrophoresis using 10%–20% (w/v) ready-made gels (Pagel; ATTO, Tokyo, Japan) with the Laemmli buffer and electroblotted to a polyvinylidene difluoride membrane (Millipore, Billerica, MA). Primary antibodies were goat polyclonal carbonic anhydrase I (CAI) antibody (Millipore, Billerica, MA) and mouse monoclonal antibody against human complement C3b-α (PROGEN, Heidelberg, Germany). The membrane was incubated with the primary antibodies and then with the relevant horseradish peroxidase (HRP)-conjugated anti-goat or anti-mouse IgG as described previously [18]. Blots were developed using an enhanced chemiluminescence plus detection system (GE Healthcare, Buckinghamshire, UK).

2.6. Enzyme-Linked Immunosorbent Assay (ELISA). To develop sandwich ELISA, the capture antibody (rabbit polyclonal CAI antibody, Abnova, Taipei, Taiwan) was immobilized on a 96-well plate (Thermo Fisher Scientific, MA) at a final concentration of 2.5 μg/mL and incubated at 4°C overnight. A mouse monoclonal CAI antibody (0.5 μg/mL; Abnova, Taipei, Taiwan) was used as the detection antibody. After incubation with HRP-conjugated goat anti-mouse IgG (Vector Laboratories, Burlingame, CA) for 1 h and then with

Table 1: Clinicopathological characteristics of individuals examined in this study.

		All cases ($n = 162$)						Cases analyzed by 2DICAL ($n = 40$)		
		PCa* ($n = 54$)	BPH ($n = 22$)	Prostatitis ($n = 6$)	RCC ($n = 20$)	Healthy ($n = 60$)	P value	PCa* ($n = 25$)	Healthy ($n = 15$)	P value
Age	(mean ± SD)	66. 3 ± 7.3	72.3 ± 7.5	65.8 ± 5.9	63.8 ± 8.5	67.2 ± 8.8	0.544****	67.0 ± 7.2	65.1 ± 8.0	0.440****
Stage	I	0						0		
	II	50						22		
	III	2						2		
	IV	2						1		
TNM classification**	T1cN0M0	25						10		
	T2aN0M0	15						7		
	T2bN0M0	2						1		
	T2cN0M0	8						4		
	T3aN0M0	2						2		
	T4N0M1b	1						1		
	T4N1M1b	1						0		
PSA***	ng/mL									
	<4	2	11	4		51		2	12	
	4≦, ≦10	30	10	2		9	<0.001*****	14	3	<0.001*****
	10<	22	1	0		0		9	0	
Gleason score	5	2						1		
	6	15						7		
	7	25						12		
	8	8						4		
	9	2						1		
	10	2						0		

*Abbreviation: PCa: prostate cancer; **according to TNM Classification of Malignant Tumors (International Union Against Cancer), 6th Edition; ***measured by Tandem R kit before the first treatment; ****Welch's t-test; *****Fisher's exact test.

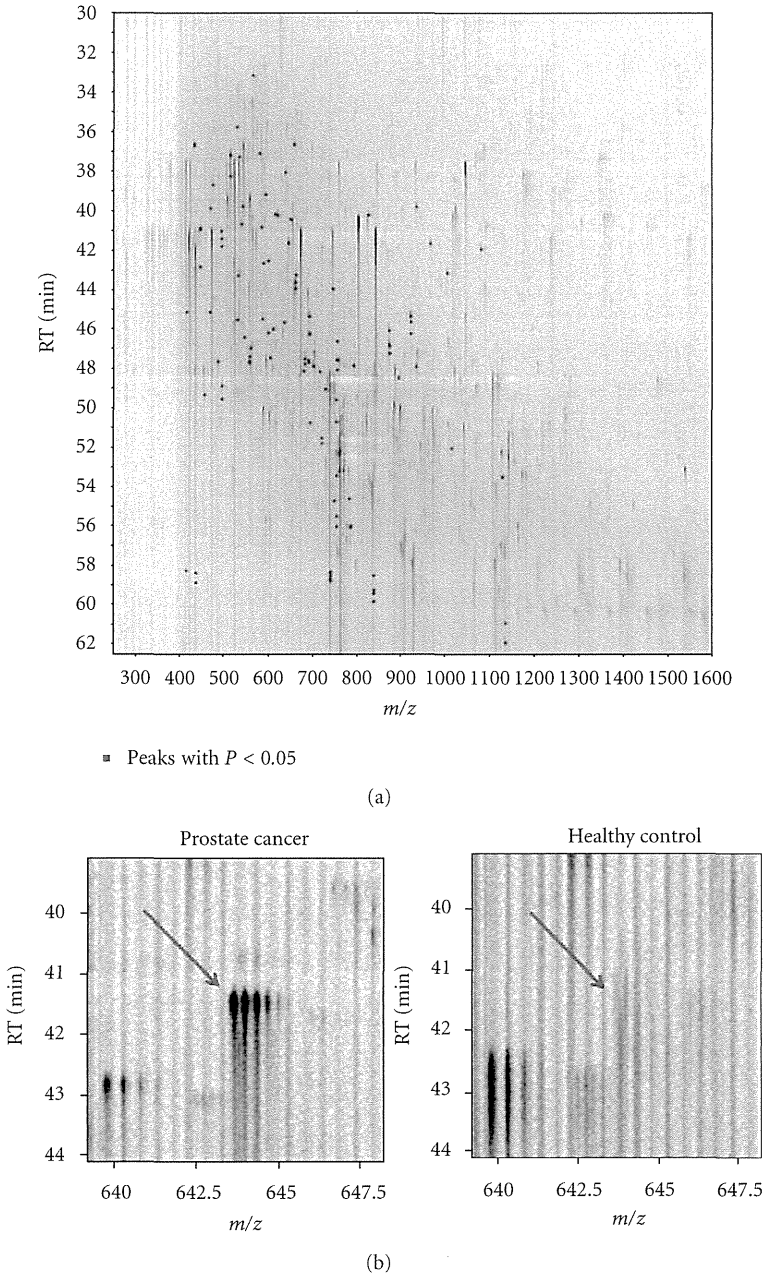

FIGURE 1: (a) Two-dimensional display of all MS peaks. The 117 MS peaks whose mean intensities significantly differed between prostate cancer patients and healthy controls ($P < 0.05$, Welch's t-test) are highlighted in red. RT: retention time. (b) 2DICAL images of peak ID 396 in a representative prostate cancer patient (left) and a healthy control (right).

OPD solution for 10 min, absorbance was measured at 490 nm using EnSpire AlphaPLUS (PerkinElmer, Waltham, MA).

2.7. Cell Lines. The human prostate cancer cell line 22Rv1 was purchased from Riken BRC Cell Bank (Tsukuba, Japan) and cultured in Roswell Park Memorial Institute Medium 1640 supplemented with 10% fetal bovine serum. Normal human prostate epithelial cells (CC-3165 PrEBM) were purchased from Lonza (Basel, Switzerland). The cells were cultured at 37°C under 5% CO_2. The culture medium was changed every 3 days. After incubation of cell lines for 48 h, the cultured conditioned media were collected, filtered through a sterile 0.22-mm filter unit, and concentrated 100-fold by freeze drying. A 10 μL sample of concentrated medium was used for Western blot analysis.

2.8. Immunohistochemistry. Cells were seeded on BioCoat collagen I-coated 8-well culture slides (Becton Dickinson Labware, Bedford, MA) and cultured overnight. The cells were washed twice with PBS (pH 7.2) and fixed with 4% paraformaldehyde in PBS for 20 min at room temperature.

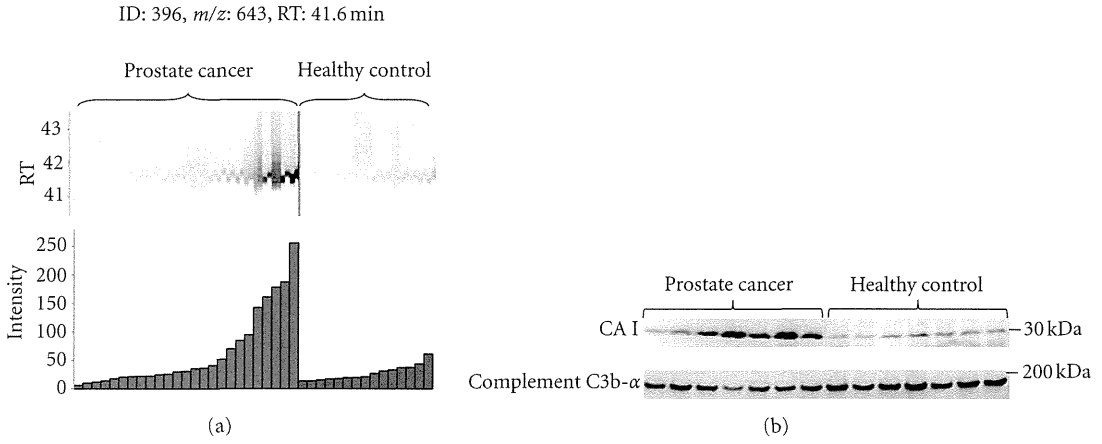

FIGURE 2: (a) MS peaks of peak ID 396 in triplicate LC-MS runs (25 with prostate cancer (left) and 15 with healthy controls (right)) aligned along LC RT. Columns represent the mean intensities of triplicate runs. (b) Immunoblotting of CAI and complement C3b-α (loading control) for 7 prostate cancer patients selected from the most intense MS peaks and 7 healthy controls from the least intense peaks.

Fixed cells were permeabilized with 0.1% Triton in PBS for 5 min, washed 3 times with PBS, blocked for 30 min with 5% normal donkey serum (Chemicon International, Inc., Temecula, CA) in PBS, and stained with the indicated primary antibodies diluted in 1% normal donkey serum overnight at room temperature. After washing 3 times with PBS, fluorophore-conjugated secondary antibodies were applied for 1 h at room temperature and washed with PBS. Alexa Fluor 568-phalloidin was used to visualize the actin cytoskeleton. The slides were mounted with Vectashield antifade reagent (Vector Laboratories), covered with glass coverslips, and observed under Zeiss LSM510 fluorescence microscope equipped with 488/514-nm argon and 543-nm helium-neon lasers.

To stain human tissues, 10 radical prostatectomy specimens were selected with five high and five low plasma CAI concentrations. Sections (4 μm) from 10% formalin-fixed paraffin-embedded material were deparaffinized in xylene and rehydrated in ethanol. Endogenous peroxidase activity was blocked by methanol containing 0.3% hydrogen peroxidase for 30 min. Microwave heating was used for antigen retrieval. The sections were incubated at 4° C overnight with a primary antibody and then incubated with a second antibody for 40 min at room temperature. The reaction products were visualized using diaminobenzidine tetrahydrochloride and counterstained with hematoxylin.

2.9. Statistical Analysis. Statistical significance of intergroup differences was assessed by the Welch's t-test and Mann-Whitney U test. Area under the receiver operating characteristic (ROC) curve (AUC) was calculated for each marker to evaluate its diagnostic significance. A composite index of 2 markers was generated using the results of multivariate logistic regression analysis, which also enabled the calculation of sensitivity, specificity, and ROC curve. Statistical analyses were performed using an open-source statistical language R with the optional module design package.

3. Results

3.1. Plasma Biomarker Discovery by Quantitative MS. To identify a diagnostic biomarker for prostate cancer patients we compared the plasma proteins of 25 prostate cancer patients with those of 15 healthy controls using 2DICAL (Table 1). Among 40,678 independent MS peaks detected within 250–1, 600 m/z, and 30–62.5 min, we found 117 peaks showing significant differences between prostate cancer patients and healthy controls ($P < 0.05$, Welch's t-test). Figure 1(a) shows a representative 2-dimensional view of all MS peaks displayed with m/z along the x-axis and LC retention time along the y-axis. The 117 MS peaks whose expression levels differed significantly between cancer patients and healthy controls are highlighted in red. MS/MS spectra acquired from these 117 MS peaks matched 4 proteins in the database with Mascot scores of >30. Ten peaks matched amino acid sequences of CAI (Table 2). The CAI-derived peak (ID 396) that clearly differed between cancer patients and healthy controls is shown as a representative peak (Figure 1(b)). The intensity distribution of peak ID 396 was different between prostate cancer patients (left) and healthy controls (right) (Figure 2(a)). Immunoblotting with a CAI probe confirmed the results of the 2DICAL findings (Figure 2(b)).

3.2. Large-Scale Validation of Plasma CAI by ELISA. To further validate plasma CAI levels in prostate cancer patients determined using 2DICAL, we performed ELISA to quantify plasma CAI levels in numerous plasma samples. The plasma samples were derived from patients suffering from prostate cancer ($n = 54$), prostatitis ($n = 6$), BPH ($n = 22$), and RCC ($n = 20$) as well as from healthy controls ($n = 60$). Plasma CAI levels were significantly different between prostate cancer patients and healthy controls ($P = 0.022$, Mann-Whitney U test). Plasma CAI levels of patients with BPH or RCC did not show significant differences from healthy

Table 2: Summary of protein identification by tandem mass spectrometry.

ID	*m/z*	RT* (min)	Charge	Normal (mean ± SD)	PCa* (mean ± SD)	*P* Values**	Mascot score	Peptide sequence	Protein description	Uniprot ID
396	643.7	41.6	3	27.35 ± 13.42	63.53 ± 67.39	0.015	95.02	HDTSLKPISVSYNPATAK	Carbonic anhydrase 1	CAH1_HUMAN
310	790.9	47.8	2	24.96 ± 9.73	62.84 ± 72.61	0.016	72.71	ESISVSSEQLAQFR	Carbonic anhydrase 1	CAH1_HUMAN
983	753.0	47.5	3	16.02 ± 4.60	30.40 ± 27.50	0.017	71.62	EIINVGHSFHVNFEDNDNR	Carbonic anhydrase 1	CAH1_HUMAN
1463	719.4	51.8	2	25.20 ± 22.26	11.26 ± 2.32	0.030	66.87	GLEEELQFSLGSK	Complement C4-A	CO4A_HUMAN
1656	872.4	46.0	2	16.99 ± 5.22	25.86 ± 19.63	0.041	66.24	LYPIANGNNQSPVDIK	Carbonic anhydrase 1	CAH1_HUMAN
311	513.8	37.2	2	37.71 ± 16.18	86.33 ± 85.17	0.010	59.09	YSSLAEAASK	Carbonic anhydrase 1	CAH1_HUMAN
798	585.3	45.4	2	21.08 ± 6.68	43.99 ± 34.82	0.004	56.32	SADFTNFDPR	Carbonic anhydrase 2	CAH2_HUMAN
278	485.8	47.6	2	40.70 ± 20.28	91.91 ± 92.78	0.013	50.23	VLDALQAIK	Carbonic anhydrase 1	CAH1_HUMAN
538	493.2	41.0	2	20.19 ± 5.79	47.30 ± 52.18	0.016	44.71	GGPFSDSYR	Carbonic anhydrase 1	CAH1_HUMAN
2429	680.4	47.5	2	27.43 ± 10.68	20.70 ± 3.90	0.032	43.87	LNDLEDALQQAK	Keratin, type II cytoskeletal 1	K2C1_HUMAN
1369	714.4	48.1	3	21.16 ± 5.02	31.96 ± 19.53	0.014	43.57	YDPSLKPLSVSYDQATSLR	Carbonic anhydrase 2	CAH2_HUMAN
916	494.3	48.9	2	12.19 ± 4.64	31.68 ± 32.02	0.006	39.1	VVDVLDSIK	Carbonic anhydrase 2	CAH2_HUMAN
747	920.8	45.3	3	14.00 ± 4.82	35.85 ± 40.39	0.013	36.65	SLLSNVEGDNAVPMQHNNRPTQPLK	Carbonic anhydrase 1	CAH1_HUMAN
1596	656.3	36.6	2	9.93 ± 2.84	19.94 ± 16.30	0.006	33.83	QSPVDIDTHTAK	Carbonic anhydrase 2	CAH2_HUMAN
3781	826.1	40.2	3	4.72 ± 0.94	9.10 ± 9.25	0.027	32.29	TSETKHDTSLKPISVSYNPATAK	Carbonic anhydrase 1	CAH1_HUMAN
1199	538.3	40.7	3	19.72 ± 3.65	30.15 ± 23.16	0.036	30.33	YSAELHVAHWNSAK	Carbonic anhydrase 1	CAH1_HUMAN

*Abbreviation: RT: retention time; PCa: prostate cancer

**Welch's *t*-test.

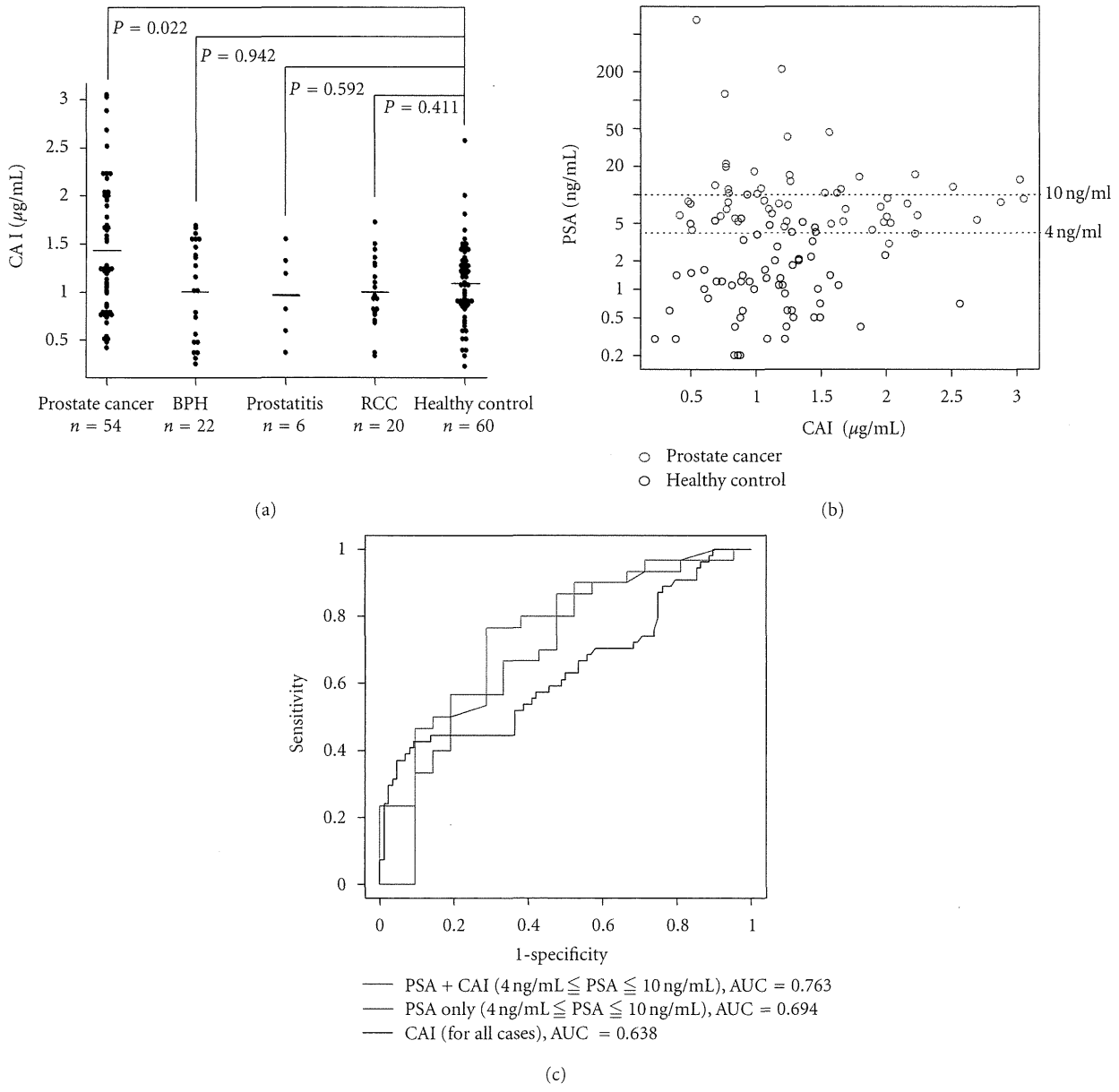

FIGURE 3: (a) Plasma CAI levels in patients with prostate cancer ($n = 54$), BPH ($n = 22$), prostatitis ($n = 6$), and RCC ($n = 20$) and healthy controls ($n = 60$) were 1.43 ± 0.69, 1.03 ± 0.51, 0.98 ± 0.46, 0.99 ± 0.36, and $1.09 \pm 1.82\,\mu$g/mL (mean ± SD), respectively. There was a significant difference between prostate cancer patients and healthy controls ($P = 0.020$, Mann-Whitney U test). Horizontal lines represented the average levels. (b) Scatter plot correlating PSA and CAI levels in prostate cancer patients (red) and healthy controls (black). The dotted lines were added to indicate the PSA gray zone. Serum PSA levels were measured using the Tandem-R kit before the first treatment in each patient. (c) ROC curve of PSA plus CAI (red line) and PSA alone (blue line) confined to the cases with PSA levels in the gray zones. ROC curves were created using a composite index of the 2 markers generated from the results of multivariate logistic regression analysis. As a reference, ROC curves of CAI (black line) for all cases were included.

controls. Plasma CAI levels of prostate cancer patients were clearly higher than those of any other patients (Figure 3(a)).

3.3. Combination of Plasma CAI Levels and PSA Assays. To determine whether plasma CAI levels and PSA assays together would be useful for diagnosing prostate cancer, CAI and PSA levels from the same cases were compared (Figure 3(b)). Pearson's CC between them was −0.106, which meant that these 2 proteins had different vectors in blood concentration. From the distribution data in the plot, CAI levels in prostate cancer patients with PSA levels of >20 ng/mL were low and CAI levels were higher in prostate cancer patients with PSA levels in the gray zone, compared to healthy controls.

To understand the diagnostic significance of CAI levels that coincided with PSA levels in the gray zone, subjects